ELSEVIER

Journal of Hydrology 237 (2000) 113–125

Journal of Hydrology

www.elsevier.com/locate/jhydrol

Subsurface drainage from hummock-covered hillslopes in the Arctic tundra

W.L. Quinton[a,*,1], D.M. Gray[b], P. Marsh[a]

[a]*National Hydrology Research Centre, 11 Innovation Blvd., Saskatoon, Canada S7N 3H5*
[b]*Division of Hydrology, University of Saskatchewan, Saskatoon, Canada S7N 0W0*

Received 28 July 1999; revised 18 July 2000; accepted 18 July 2000

Abstract

In the Arctic tundra, subsurface drainage occurs predominantly through the saturated zone within the layer of peat that mantles the hillslopes. In plan view, the peat cover is fragmented into a network of channels due to the presence of mineral earth hummocks. In cross section, the physical and hydraulic properties of the peat vary with depth and the water transmission characteristics (e.g. hydraulic conductivity) of the upper profile differ distinctly from those of the lower. Water flow through the peat is laminar, therefore the friction factor (f) and the Reynolds number (N_R) are inversely related. Average values for the coefficient C of the relation $f = C/N_R$, vary from ~300 near the surface to ~14,500 at depth. This large difference in C confirms that the larger-diameter soil pores of the living vegetation and lightly decomposed peat near the surface offer much less resistance to water motion than the finer-grained peat deeper in the profile. Also, the variability suggests that subsurface drainage is strongly affected by the position and thickness of the saturated zone within the peat matrix. A first approximation for a model or simulation of the flow regime may consider a peat profile with depth-varying, resistance properties in respect to subsurface flow.

Keywords: Subsurface runoff; Peat; Arctic tundra; Permafrost; Modelling

1. Introduction

Tundra, the treeless terrain with a continuous organic cover (NRC, 1988), occupies ~31% of the Canadian Arctic (Bliss and Matveyeva, 1992). Soil profiles in this region are typically composed of a highly permeable layer of peat (NWWG, 1988) overlying mineral sediment with a relatively low permeability. Where the organic layer overlies fine-grained, frost-susceptible soils, frost heave and cryoturbation can produce mineral earth hummocks, the most widely distributed form of patterned ground in the permafrost areas of the world (MacKay, 1980). Where these features occur, the ground surface is fragmented into areas occupied by earth hummocks, where mineral soil is at the surface, or just a few centimetres below it, and inter-hummock areas containing peat. Because of the inter-connectivity and relatively high permeability of the inter-hummock waterways, subsurface flow through the inter-hummock area is the dominant means of drainage from hummock-covered hillslopes (Quinton and Marsh, 1998, 1999a).

In recent years, much effort in modelling runoff

* Corresponding author. Tel.: +1-604-291-3715; fax: +1-604-291-5841.

E-mail address: bquinton@sfu.ca (W.L. Quinton).

[1] *Present address:* Department of Geography, Simon Fraser University, Burnaby, Canada, V5A 1S6.

0022-1694/00/$ - see front matter
PII: S0022-1694(00)00304-8

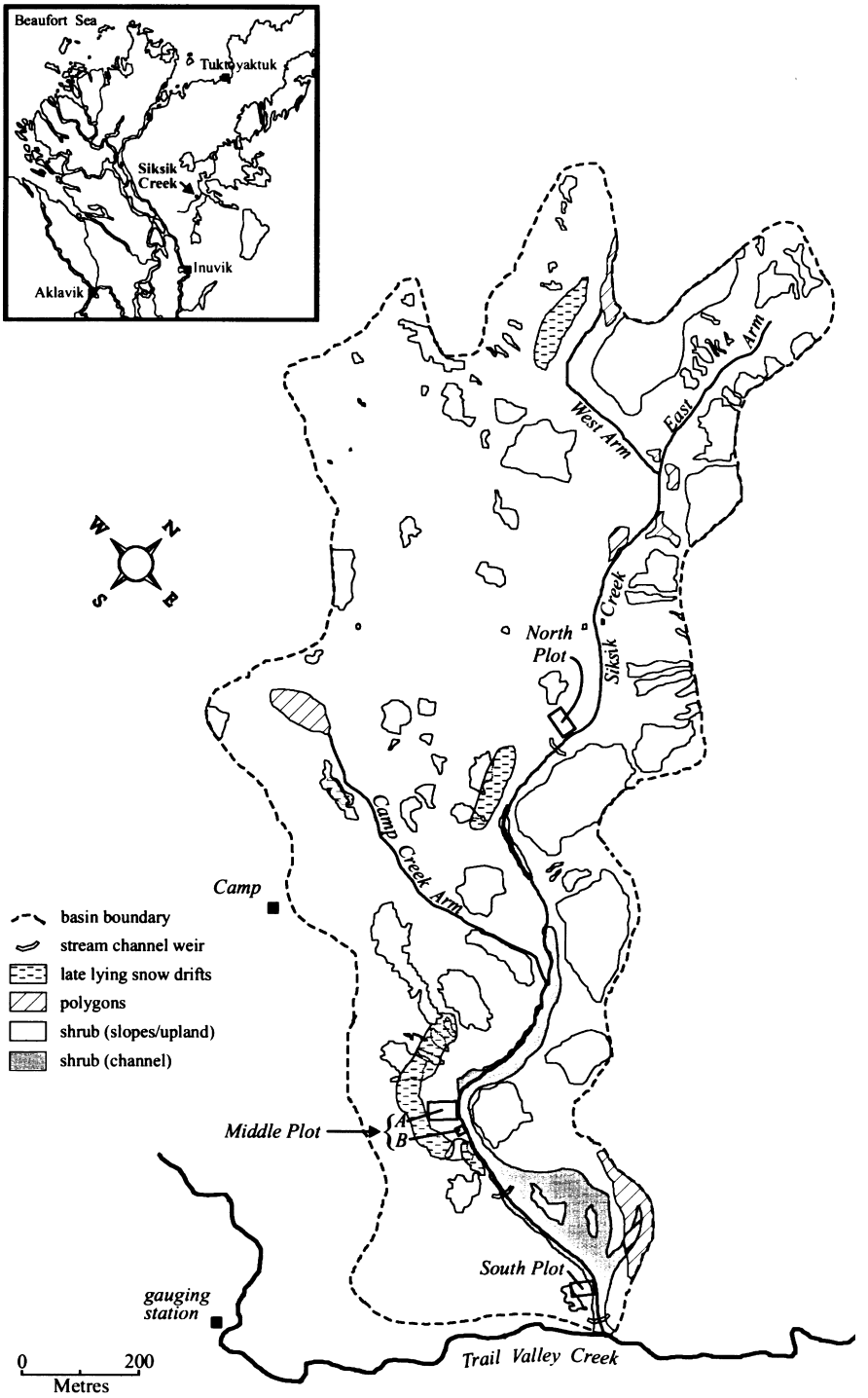

Fig. 1. The Siksik Creek basin, showing the location of the hillside study plots, and various terrain types.

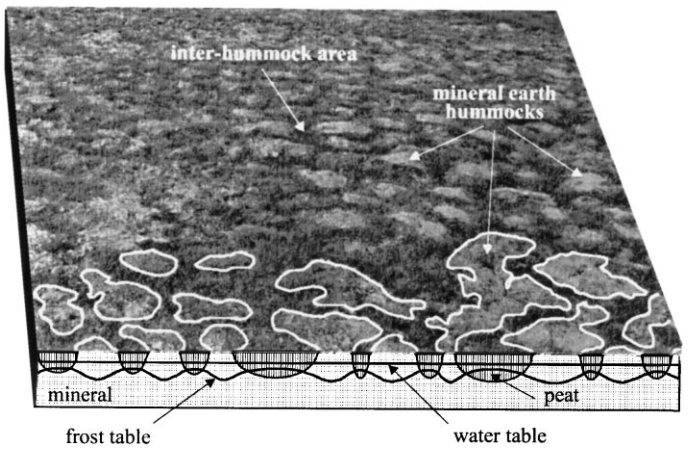

Fig. 2. A ground-level photograph showing the surface of a hummock-covered hillslope, and a schematic section across several mineral earth hummocks, inter-hummock channels, the water table and the frost table.

processes in the Arctic tundra, has focussed on the vertical flux of meltwater through snowpacks. Models based on the surface energy balance and snow metamorphism have been developed that predict vertical meltwater fluxes whose values compare well with observations (e.g. Marsh and Pomeroy, 1996). These models estimate the amount of water available for lateral drainage from hillslopes. When modelling the overall runoff pathway from the surface of a melting snowpack to the stream channel and the amount and timing of runoff water reaching stream channels, the processes controlling lateral flow must be properly represented.

A well-known approach to modelling lateral flow through melting snow is presented by Colbeck (1974). This procedure assumes: (a) a melting snow cover overlies impermeable ground, (b) flow occurs through a saturated 'slush' layer at the base of the snowpack, (c) flow can be described by Darcy's law and (d) the increase in the thickness of the 'slush layer' with distance downslope is small compared with the slope. The equation governing flow in the saturated zone is solved using a coordinate system that moves downslope at the velocity of the water particles. In the Arctic tundra, normally meltwater released by a snowcover infiltrates the ground below the snow and lateral flow occurs through the peat rather than through the base of the snowpack (Quinton and Marsh, 1999a). Despite the difference, it is surmised that Colbeck's solutions may provide reasonable estimates of subsurface, lateral flow because of the high permeability of the peat near the surface.

A better understanding of the physical and hydraulic properties of the peat matrix and of lateral flow in Arctic tundra will enhance the development of a hillslope runoff model for an environment where well over half of the cumulative annual discharge is generated by snowmelt. The objectives of this paper are: (a) to present the results of a field study of subsurface runoff from arctic tundra hillslopes during snow ablation and ground thawing; (b) to examine the effects of variations in soil hydraulic properties and the position and thickness of the saturated layer on water movement; and (c) to recommend an approach for modelling hillslope runoff.

2. Study site

The study was conducted at Siksik Creek (68° 44′N, 133° 28′W) located approximately 55 km north–northeast of Inuvik, and 80 km south of Tuktoyaktuk on the Arctic Ocean (Fig. 1). The watershed is located at the northern fringe of the forest-tundra transition zone (Bliss and Matveyeva, 1992), and is within the continuous permafrost zone (Heginbottom and Radburn, 1992). Siksik Creek drains a 95.5 ha area with elevations ranging between approximately 60 and 100 m asl.

Mineral earth hummocks occur throughout the

study basin and cover between 30 and 70% of hillslope surfaces (Fig. 2). Their diameters range between 40 and 100 cm, with crests rising 10–40 cm above the surrounding inter-hummock surface. The hummock surfaces are bare or support a thin layer of lichen (*Alectoria* and *Cladina* spp). The inter-hummock vegetation consists of sedges (*Eriophorum* and *Carex* spp) and small vascular plants *(Empetrum, Vaccinnium, Ledlum*and *Rubus* spp) rooted in a continuous cover of moss (*Sphagnum* spp). The peat in the inter-hummock area has an overall thickness between ~0.3 and 0.5 m. The upper ~0.1–0.2 m is composed of living vegetation and lightly decomposed peat. Below this, the peat is moderately to strongly decomposed (Quinton and Marsh, 1999a). This layered peat profile resembles that found in wetlands possessing acrotelm and catotelm layers (Ingram, 1978). Strictly speaking, the lower peat layer in the tundra setting should not be thought of as a catotelm, since, by definition, the catotelm has "a constant or little changing water content" (Ivanov, 1981, p. 58), while at the study site, particularly in upland areas, the water table was found to drain away from the peat profile as thawing progressed (Quinton and Marsh, 1999a).

The inter-hummock area is composed of inter-hummock channels that form the hillslope drainage network. Some inter-hummock channels contain soil pipes, whose diameters range between 5 and 10 cm. Pipes are generally <1 m in length, therefore over the length of a hillslope (i.e. tens of metres), pipe flow is inter-connected with matrix flow, with the flow rate limited by the transmission properties of the peat matrix. Pipes occur primarily in the lower peat layer, with the upper layer forming a peat 'roof'. They are common on hillsides with slopes $> \sim 0.08$, but do not occur on slopes $< \sim 0.04$. By late summer, the average frost table depth was ~30 cm in the inter-hummock area, compared with ~60 cm in the hummocks (Quinton and Marsh, 1998). Underlying the organic cover throughout the basin are fine grained, frost susceptible soils.

The climate at Siksik Creek, as inferred from the climate normals for Inuvik and Tuktoyaktuk (AES, 1982a; AES, 1982b), is characterised by short, cool summers and long cold winters, with eight months of snow cover. The mean daily temperature rises above 0°C in early June, and falls below 0°C in early October, with a mean annual air temperature of −9.8°C at Inuvik and −10.9°C at Tuktoyaktuk. The mean annual precipitation totals at Inuvik (266 mm) and Tuktoyaktuk (138 mm) are comprised of 66 and 47% snowfall, respectively. Monthly precipitation is greatest in August, September and October, with most precipitation falling as rain in August and September, and as snow in October.

3. Methodology

Hydrological measurements were made at four small (~1000–2000 m^2) experimental plots: North, Middle-A, Middle-B and South plots in 1993 and 1994 (Fig. 1). At each plot, snow pits with a surface area of ~0.25 m^2 were excavated prior to and during snow melt in order to observe whether basal ice was present, and if water moved laterally downslope at the base of the snow. Each pit was covered with a plywood board with a reflective surface in order to limit warming and melt within the snow pit. In the inter-hummock area, the depths of the water table and the frost table below the ground surface were measured daily at various distances from the stream edge. The water table depth was measured manually at observation wells (6 cm inner-diameter), and the depth of the frost table was measured with a graduated steel rod at fixed points along a transect. The infiltration rate into the inter-hummock peat was measured using a falling-head, ring infiltrometer.

Tracer tests were conducted at Middle Plot-A and Middle Plot-B in 1993, and at the North and South plots in 1994. For each tracer test, approximately 80 l of KCl solution (~100 mg l^{-1} Cl^{-1}) was poured onto the ground surface along a ~10 m line traversing each plot, at a distance of ~10 m up slope of the stream bank. Tracer concentrations were measured in eight, roughly evenly spaced inter-hummock channels at each plot, using chloride sensing micro-electrodes (Farrell et al., 1991; Quinton and Marsh, 1999b) inserted into the peat matrix to a depth corresponding to the middle of the saturated zone. The sensors were connected to a data logger with readings made every 60 s and averaged and recorded every 15 min. No surface flow was observed between the tracer application line and the stream bank during a test. The tracer tests were repeated at different times throughout the

Table 1
The average percentage sand (0.05–2.0 mm), silt (0.002–0.05 mm) and clay (<0.002 mm) class sizes composing the soils sampled from various depths, *d*, below the surface of mineral earth hummocks

d (m)	sand%	silt%	clay%
0.1	30.2	34.9	34.8
0.15	47.9	26.4	25.7
0.2	34.1	39.5	26.4
0.3	26.6	38.5	36.9

development of the active layer in order to obtain estimates of the saturated hydraulic conductivity for different elevations of the saturated zone within the peat profile. In both years of the study, the first tracer test was conducted less than a week after the ground surface between the application line and the stream bank became snow-free.

The saturated hydraulic conductivity was computed from measurements taken in the tracer tests by the expression:

$$k = \eta_A v \left(\frac{dh}{dx} \right)^{-1}, \quad (1)$$

where η_A is the active porosity of the inter-hummock pea; v, the average velocity of flow through the active pores; and dh/dx, the hydraulic gradient between the application line and the sensor location.

The average pore velocity was computed as:

$$v = \frac{L_X}{t_C} T_X, \quad (2)$$

where L_X is the straight line distance between the tracer application line and sensing electrode; t_C, the length of time between the time of application of the tracer and the time when the centre of mass of the tracer plume reached the sensor; and T_X, the ratio of average length of the flow path between the tracer application line and sensing electrode, L, to the straight line distance, i.e. $T_X = L/L_X$ (Quinton and Marsh, 1999b). T_X, the average tortuosity of the inter-hummock channels, is a measure of the increase to the flow distance due to the mineral earth hummocks. At Siksik Creek, T_X ranged between 1.1 and 1.5, and the average value for each plot was taken from Quinton and Marsh (1998).

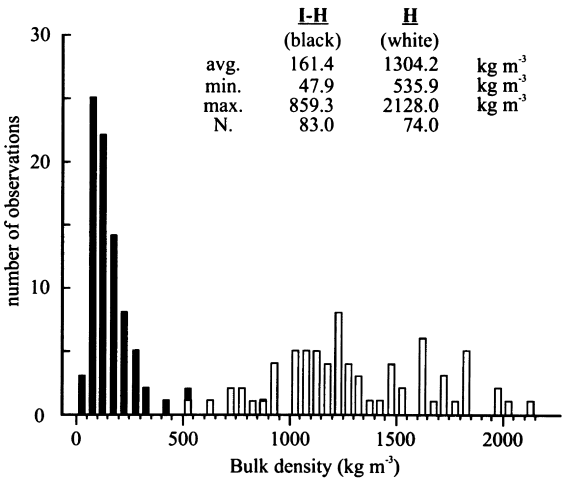

Fig. 3. Frequency distribution of bulk density of surface soils (0–5 cm below ground surface) sampled from the inter-hummock area (I-H) and from earth hummocks (H).

At Middle Plot-A, pump tests were conducted at two wells, one located on the crest of a hummock (mineral soil), and the other at an adjacent point in the inter-hummock area (peat). The hydraulic conductivity of the material was calculated from these data using the formula for a fully-penetrating well into an unconfined aquifer, described by Bouwer (1989). Soil cores were taken from the inter-hummock area of each plot and the hydraulic conductivity determined from tests conducted with a constant head permeameter. The cores were extracted using 10×30 cm sections of PVC pipe inserted vertically into the peat surface. The permeameter was designed so that the soil samples remained in the tubes during the hydraulic conductivity tests. The specific yield of the peat in the soil cores was measured following the procedure described by Boelter (1976).

Gravimetric samples of near-surface soils (upper 5 cm) were taken to determine bulk density. Core samples containing the entire peat profile (~30–40 cm) were extracted for determinations of bulk density, total porosity, active porosity (i.e. the proportion of the total peat pore volume that actively transmits water (Romanov, 1968)) and the geometric mean pore diameter. All cores were sampled from within a 10×10 m^2 area, within Middle Plot-A. Bulk density

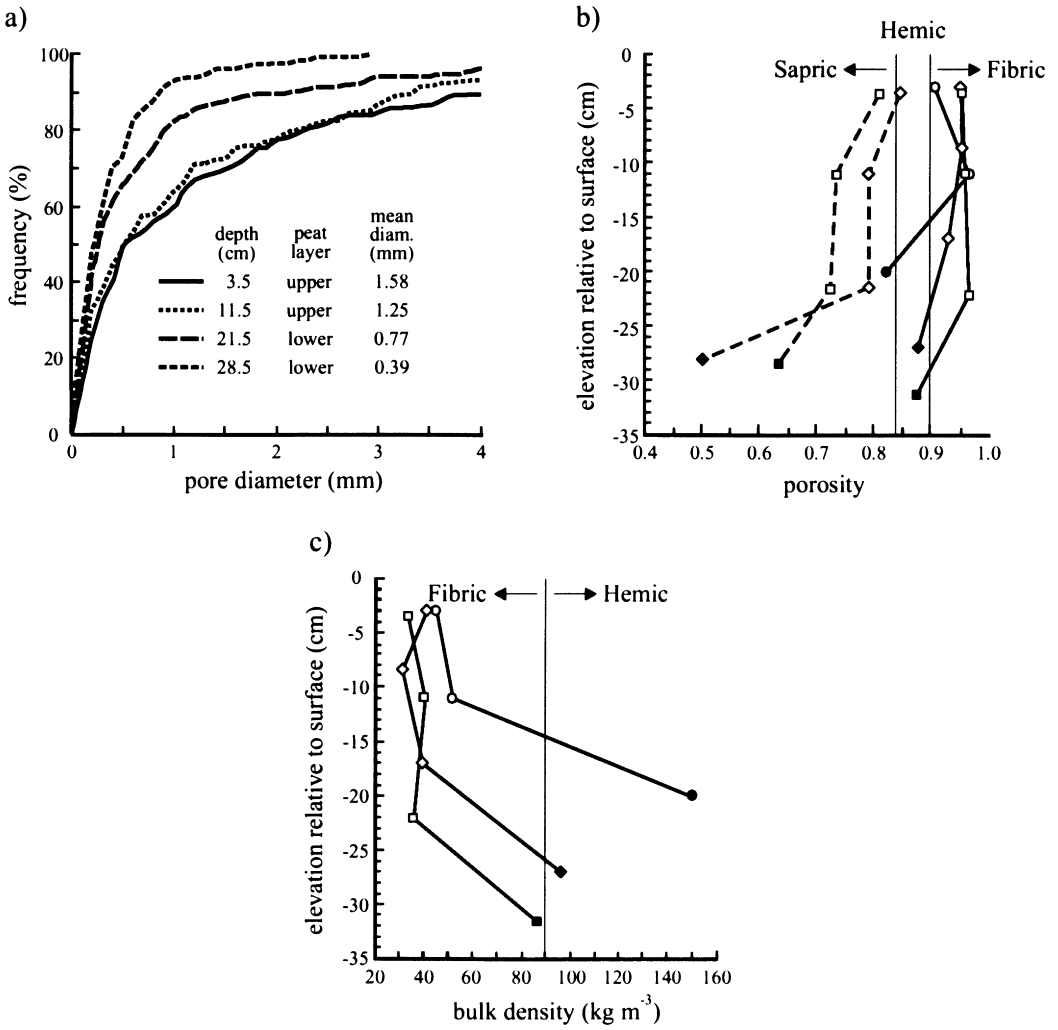

Fig. 4. (a) The cumulative frequency distribution of pore diameters for pores less than 4 mm diameter at four depths below the ground surface. The upper two depths (3.5 and 11.5 cm) are in the upper peat layer, and the lower two (21.5 and 28.5 cm) are in the lower peat layer; (b) variations in total (solid lines) and active (dashed lines) porosity for three peat cores; and (c) variations in bulk density with depth. In (b) and (c) open and solid symbols denote samples taken from the upper and lower peat layer, respectively. Also shown in (b) and (c) are the stages of decomposition (fibric, hemic, sapric) based on the total porosity and bulk density values (Verry and Boelter, 1978).

and total porosity were obtained by the procedure described by Boelter (1976). The active porosity, η_A, of the peat was determined by image analyses of photographs of thin sections (~100 μm thick). This procedure involved determining the percentage void space (interparticle pores) on five representative 1 cm^2 windows at each sampling depth. An average value of η_A for each depth was then calculated. The active porosity is a smaller value than the total porosity, since the latter also includes the porosity of the peat particles. This "inactive" porosity is composed of closed and dead-end pores formed by the remains of plant cells (Hoag and Price, 1997). The geometric mean pore diameter for each depth was computed from measurements of pore diameters from image analysis of thin soil sections. This calculation involved the diameters of 100–150 pores along each of five evenly spaced transects of a section. The

Table 2
The hydraulic conductivity, k (m d^{-1}), measured with a constant head permeameter, and specific yield, S_Y (volume fraction), of soil cores sampled from the inter-hummock area

Sample	1	2	3	4	5	6	7	8	9	Average
k	14.81	2.83	43.38	66.15	2.58	45.32	98.51	110.2	26.91	45.64
S_Y	0.23	0.24	0.23	0.34	0.36	0.26	0.24	0.26	0.26	0.27

resolution of the images prevented detection of pores with diameters less than approximately 16 μm.

4. Results and discussion

4.1. Soil textural properties

The mineral material on the hillslopes is fine-grained, with a large clay-sized fraction and there is relatively small variation in the particle size distribution with depth (Table 1). On average, the bulk density of the surficial (0–5 cm) material is approximately 1000 kg m^{-3} higher in the hummocks than in the inter-hummock area (Fig. 3). The division of hillslope soils into areas of high (hummock) and low (inter-hummock) bulk density, results in preferential flow through the inter-hummock area.

Within the inter-hummock channels, the relative proportion of small pores in a sample increases with increasing depth below the surface (Fig. 4a). Likewise, the total porosity, the active porosity and the bulk density change with depth. In Fig. 4b, the total porosity is shown for three peat profiles, and the active porosity for two of them. One core was relatively small, and therefore had only three measurements of total porosity. The active porosity of the peat near the ground surface approached 0.8, but decreased at depth to between 0.5 and 0.63. The more abrupt decrease in the active porosity than in the total porosity at depth suggests a decrease in pore size and a higher proportion of closed and dead end (i.e. inactive) pores at depth (Hoag and Price, 1997). Bulk density increased from approximately 40 kg m^{-3} near the surface to between 84 and 150 kg m^{-3} in the lower peat (Fig. 4c).

Fig. 4 demonstrates the difference in the physical properties of the upper and lower peat layers, and shows that the thickness of these layers varies widely over the relatively small (i.e. 10×10 m^2) area of the hillslope from which the cores were collected. From the one-dimensional view of a soil profile, there is a distinct boundary between the upper and lower peat layers, giving the impression that as the water table moves across this boundary, subsurface flow would shift between high and low rates. However, the large spatial variations in the thickness of these layers, in the depth to the frost table, and in the thickness of the saturated layer dampen this effect and water encounters both soil layers as it flows laterally to the stream bank.

4.2. Field observations of subsurface flow

Visual observations of runoff taken from snow pits during melt indicated that lateral, subsurface flow started after water had infiltrated the peat and occurred below the snowpack. The average infiltration rate (from infiltrometer measurements) into the inter-hummock peat was 197.3 m d^{-1}, which is in close agreement with the value of 188.4 m d^{-1} reported by Dingman (1973), for tundra in central Alaska. Given the high infiltrability of the surficial material it is unlikely that natural events would produce application rates sufficient to promote ponding or surface runoff on sloping tundra, except for conditions where the frost or water table fell close to the ground surface. Also, because of the high infiltrability and the relatively short length of the vertical pathway between the ground surface and the water table ($<$10–30 cm), it is likely that lateral subsurface movement controls the pathway and delivery of runoff to a stream channel.

4.3. Hydraulic conductivity

The results of the pump tests showed that the average hydraulic conductivity of the ~20 cm thick saturated zone is three orders of magnitude higher in the inter-hummock peat (6.1 m d^{-1}) than in the hummocks (4.7×10^{-3} m d^{-1}). This average value of 6.1 m d^{-1} for the inter-hummock area is less than

Table 3
Summary of data used to solve Eqs. (1) and (2) and for the construction of Fig. 7. t_C, average difference between the tracer application time and the time when the centre of mass of the tracer plume reached the sensors (days); L_X, average straight-line distance between the tracer application line; and the sensor (m); η_A, active porosity; dh/dx, hydraulic gradient; and T_X, tortuosity

	North (L_X, 8.310; T_X, 1.282)			Middle-A (L_X, 7.340; T_X, 1.219)			Middle-B (L_X, 5.110; T_X, 1.219)			South (L_X, 5.000; T_X, 1.327)		
Exp.	η_A	dh/dx	t_C	η_A	dh/dx	t_C	η_A	dh/dx	t_C	η_A	dh/dx	t_C
1	0.800	0.035	0.341	0.790	0.066	0.204	0.790	0.150	0.083	0.790	0.036	0.279
2	0.740	0.034	0.938	0.780	0.072	0.340	0.780	0.150	0.082	0.770	0.033	1.766
3	0.720	0.037	7.804	0.770	0.068	0.757	0.770	0.150	4.052	–	–	–
4	–	–	–	0.690	0.067	11.557	0.690	0.150	3.146	–	–	–
5	–	–	–	0.590	0.076	25.410	0.610	0.150	20.190	–	–	–

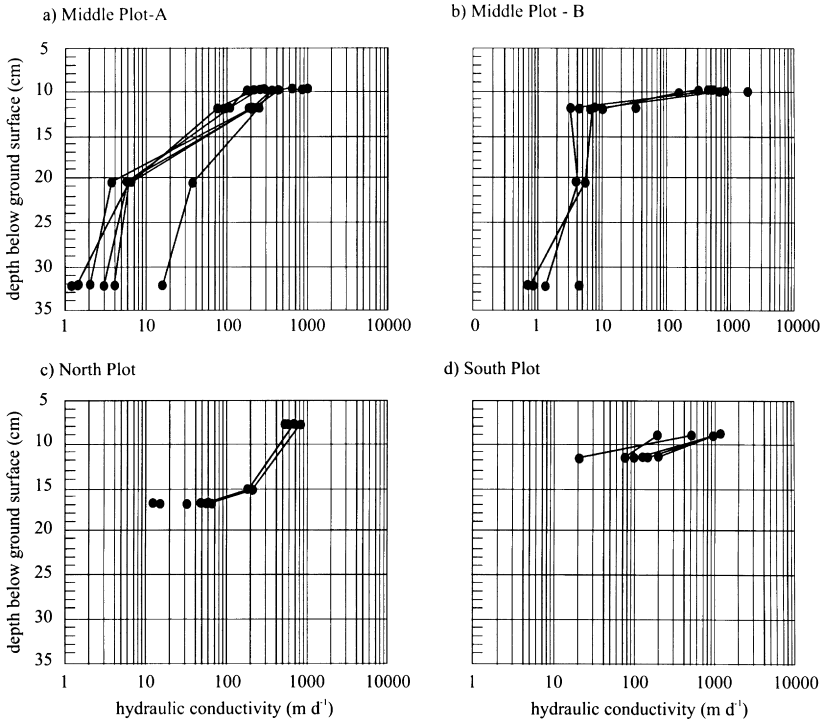

Fig. 5. The variation in hydraulic conductivity with depth in the inter-hummock area measured from the tracer tests. The data points indicate the centre of the saturated zone where the sensors were positioned.

the average value of 45.6 m d^{-1} calculated from the permeameter tests (Table 2). The large variations in average conductivity determined by the different procedures is not uncommon and likely reflect differences due to the soil anisotropy, sample size, principle flow direction, methodology and other factors.

Variations in the physical properties of peat with depth result in large changes in its transmission properties (Table 3). Average values of hydraulic conductivity for the inter-hummock area determined from the tracer tests are plotted with depth in Fig. 5. The data show hydraulic conductivity decreasing with increasing depth. Between 10 and 30 cm below the ground surface, the hydraulic conductivity can decrease by 2 to 3 orders of magnitude. The data plotted on Fig. 5 represent spatially averaged values of hydraulic conductivity, since they are affected by the transmission properties of the saturated zone over the ~10 m flow distance between the tracer application line and

Table 4
Average values of the hydraulic conductivity of inter-hummock channels, k (m d^{-1}), for various depths, d, below the ground surface. The depths provided represent the middle of the saturated zone at the time of the tracing experiments

	North		Middle-A		Middle-B		South	
Exp.	d(cm)	k	d(cm)	k	d(cm)	k	d(cm)	k
1	7.7	666.83	9.7	598.38	9.7	476.56	9	761.29
2	15.3	198.74	9.9	301.68	9.9	785.52	11.5	116.34
3	16.8	39.57	11.9	153.9	11.9	11.4	–	–
4	–	–	20.5	13.34	20.5	4.98	–	–
5	–	–	32.2	4.53	32.2	1.83	–	–

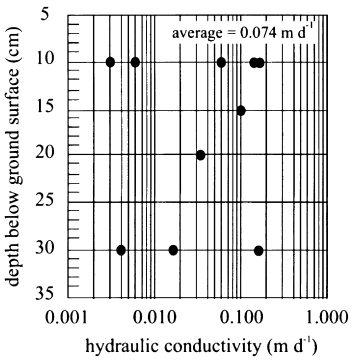

Fig. 6. Hydraulic conductivity computed from particle size on mineral soils sampled from various depths. The vertical axis shows elevation relative to the ground surface.

sensor. It is likely they strongly reflect the hydraulic properties of the least permeable material encountered along this flow length.

The average conductivity of the peat in the inter-hummock channels near the bottom of the profile (Table 4) are two to three orders of magnitude higher than the hydraulic conductivity of the mineral material (i.e. in the hummocks and below the inter-hummock peat) estimated from pump tests and particle size analysis. A comparison of the data in Figs. 5 and 6, show that the hydraulic conductivity of the mineral material is lower, has a narrower range of values, and appears independent of depth below the ground surface. The difference between the highest hydraulic conductivity in Fig. 5 and the lowest values in Fig. 6, suggests that when the water table is close to the ground surface, the hydraulic conductivity near the top of the saturated zone can be six orders of magnitude higher in the inter-hummock area than in the hummocks.

4.4. Degree of decomposition

The changes in the physical and hydraulic properties of the peat with depth below the ground surface result from the increasingly advanced state of decomposition of the peat. Based on the limits of total porosity and bulk density used by Verry and Boelter (1978), the peat is fibric (porosity > 0.9, bulk density < 90 kg m^{-3}) in the near surface, and hemic (porosity 0.84–0.9, bulk density 90–200 kg m^{-3}) at depth (Fig. 4c). Sapric peat (porosity < 0.84, bulk density > 200 kg m^{-3}) appeared in only one of the peat cores (Fig. 4b). Peat in an advanced state of decomposition was often observed at the bottom of the peat profiles. The data in Table 2 show that the average hydraulic conductivity of the upper 30 cm of the peat profiles subjected to permeameter tests, is similar to that for fibric mosses (>1.3 m d^{-1}), while the average specific yield is within the hemic range (0.1–0.45) (Verry and Boelter, 1978).

4.5. The subsurface flow regime

The effects of changes in hydraulic conductivity, water table position and depth of the saturated zone on water flow were studied by analysing the relationship between the friction factor, a measure of the resistance to flow (f) and the Reynolds number (N_R). Graphs of these variables, known as Stanton or Moody diagrams, are used in hydraulics to differentiate laminar and turbulent flow.

According to Weisbach (Rouse and Ince, 1957), the loss of hydraulic head (Δh) by a moving fluid in a pipe is directly related to the length of the pipe (L) and the velocity head ($v^2/2g$, where g is acceleration due to gravity) and inversely proportional to the diameter of the pipe (D). That is:

$$\Delta h = f \frac{L}{D} \frac{v^2}{2g}. \tag{3}$$

Combining Eq. (3) with the expression for Δh by Darcy's Law:

$$\Delta h = \frac{v\mu L}{K\rho g}, \tag{4}$$

where K is the soil permeability; ρ and μ, the density and dynamic viscosity of water; and g, the acceleration due to gravity, leads to an expression for the friction factor as:

$$f = \frac{2D^2}{K} \frac{1}{N_R} = \frac{C}{N_R}, \tag{5}$$

in which the Reynold's number, $N_R = \rho D v/\mu$ and C is a coefficient. Eq. (5) shows that $C = 2D^2/K$. Soil permeability depends only on the properties of medium, e.g. the size, shape, number, distribution and continuity of the conducting pores. Freeze and Cherry (1979) suggest the approximation, $K = cD^2$,

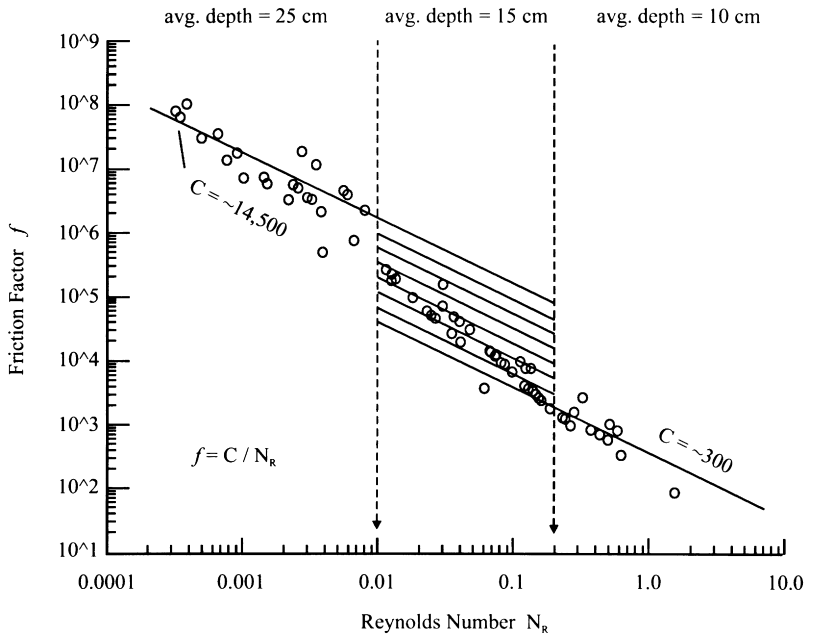

Fig. 7. The friction factor (f) plotted with the Reynolds number (N_R). The average depth of the measurement points within each Reynold's number range is identified. The solid lines for the ranges $N_R > 0.2$ and $N_R < 0.01$, are best-fit lines, and have a slope of -1, indicating laminar flow. In the range $0.01 < N_R < 0.2$, several solid lines are shown, indicating that laminar flow prevails, although the value of C is in transition.

where c, dimensionless coefficient and D, pore or grain diameter.

For laminar flow in a small, circular capillary tube, the Hagen–Poiseuille relationship gives $K = D^2/32$; therefore, $C = 64$ and Eq. (5) reduces to the well-known expression describing the relationship between f and N_R for laminar flow in pipes:

$$f = \frac{64}{N_R}. \tag{6}$$

Emmett (1979) summarises the results of tests conducted by the Hydraulics Laboratory of the US Geological Survey on uniform overland flow over impervious plane surfaces. These results suggest that for laminar flow in a smooth rectangular channel, $f = 96/N_R$, in which the pore diameter is replaced by $4y$, where y is the depth of overland flow. Todd (1959) studied the f–N_R relationship of a large number of groundwater flows using the mean grain size as the length dimension. He found that for laminar flow, $f = 1000/N_R$.

In pipe hydraulics, it is generally accepted that when N_R exceeds a value of about 2000, Eq. (6) does not apply as flow becomes turbulent and f is independent of N_R. The Reynold's number criterion to define an upper limit of laminar flow in porous materials has also been tested but the application is difficult because the matrix usually comprises a complex network of small openings or interstices, each having a different size, geometry, tortuosity and continuity. Todd (1959) reported that f decreased with N_R in the laminar range ($N_R < 10$), and is independent of N_R when flow is fully turbulent ($N_R > 1000$).

Fig. 7 is a logarithmic plot of f versus N_R calculated from the tracer measurements from all study plots, using the average pore velocity (Eq. (2)) and the geometric mean pore diameter of the saturated zone of the inter-hummock peat. All data are in the laminar flow regime and each point falls on a line defined by Eq. (5) and has a specific value for the coefficient, C. The data were subdivided based on the observation that the f-values at the ends of the plot, i.e. for $N_R < \sim 0.01$ and $N_R > \sim 0.2$, show smaller variations among values and trend toward common log-linear relationships between f and N_R. These two groups of

points correspond roughly to flows monitored at average depths of 10 cm ($N_R > \sim 0.2$) and 25 cm ($N_R < \sim 0.01$), respectively. Representative values of C for these layers are ~300 ($D = 0.54$ mm) and ~14,500 ($D = 0.27$ mm).

The large difference between values for C for the top and bottom of the peat confirms that the resistance to water motion is much less in the larger-diameter soil pores of the peat near the surface than in the finer-grained material near the bottom of the profile and that the flow regimes vary widely over the wetted profile. As the ground thaws, and saturated zone descends through the peat profile, the resistance to motion increases and the value for C increases. Between the values of $C = \sim 300$ and 14,500 (Reynold's number range: $0.01 \leq N_R \leq 0.2$) the variations in f and C reflect the interactions between the saturated zone elevation and thickness, and the large vertical gradients and variations in the water-conducting properties within the matrix. Over this range, it appears there is a trend for $\ln f$ to vary linearly with depth. Based on these findings a first approximation for a model or simulation of the flow regime may consider the peat profile as a single, continuous layer with depth-varying resistance properties.

5. Conclusions

In the Arctic tundra, preferential subsurface flow from hillslopes occurs through inter-hummock channels that form the drainage network. The layer of peat in the inter-hummock channels generally is between 0.3 and 0.5 m thick and consists of an upper mantle of living material that changes to moderately to strongly decomposed peat at depth. Similarly, the bulk density of the peat increases with depth, whereas the mean pore diameter, the total porosity and the active porosity decrease. These variations in physical properties cause large changes in the hydraulic properties of the material with depth. For example, the average hydraulic conductivity at 9 cm is 2 orders of magnitude greater than the average conductivity at 26 cm, 625.8 m d^{-1} compared to 6.2 m d^{-1}.

Lateral movement of subsurface through the unfrozen layer of peat during runoff is laminar and can be described by the Darcy–Weisbach expression, $f = C/N_R$, where f is the friction factor; C, a coefficient; and N_R, the Reynolds number. When the saturated zone is confined within either the surface material or the deeper, decomposed peat, C tends to reasonably constant values equal to $C = 300$ ($N_R > \sim 0.2$) and $C = \sim 14,500$ ($N_R < \sim 0.01$), respectively. Conversely, when the saturated zone overlaps the layers of living and decomposed peat and $0.01 \leq N_R \leq 0.2$ there is a trend for $\ln f$ to vary linearly with depth. The findings suggest that the flow regime may be analogous to the movement of water a through a single, continuous layer of peat with depth-varying resistance properties.

Acknowledgements

The authors wish to thank Cuyler Onclin, Brenda Sørensen and Carolyn Teare for their assistance in the field, and Dr Ahmet Mermut for his assistance in the preparation of soil thin sections. Financial support was provided by the National Water Research Institute (Department of Environment), the University of Saskatchewan, the Canadian GEWEX programme, the Northern Scientific Training Programme (Department of Indian and Northern Affairs). Logistical support was provided by the Polar Continental Shelf Project (Department of Energy, Mines and Resources), and the Aurora Research Institute in Inuvik. (Government of the Northwest Territories). The Authors wish to thank Prof. M.J. Kirkby and Prof. N.T. Roulet for their reviews, which contained many helpful and useful comments and suggestions.

References

Atmospheric Environment Service (AES), 1982a. Temperature 1951–1980. Canadian Climate Normals, vol. 2. Environment Canada, Toronto (306pp).

Atmospheric Environment Service (AES), 1982b. Precipitation 1951–1980. Canadian Climate Normals, vol. 3. Environment Canada, Toronto (602pp).

Bliss, L.C., Matveyeva, N.V., 1992. Circumpolar arctic vegetation. In: Chapin III, F.S., Jefferies, R.L., Reynolds, J.F., Shaver, G.R., Svoboda, J. (Eds.). Arctic Ecosystems in a Changing Climate: an Ecological Perspective, Academic Press, San Diego, pp. 59–89.

Boelter, D.H., 1976. Methods for analysing the hydrological characteristics of organic soils in marsh-ridden areas. In: Hydrology of Marsh-Ridden Areas. Proceedings of IASH Symposium Minsk., 1972. IASH, UNESCO, Paris, pp. 161–169.

Bouwer, H., 1989. The Bouwer and Rice Slug test — an update. Ground Water 27 (3), 304–309.

Colbeck, S.C., 1974. Water flow through snow overlying an impermeable boundary. Water Resources Research 10, 119–123.

Dingman, S.L., 1973. Effects of permafrost on stream flow characteristics in the discontinuous permafrost zone of central Alaska. In: Proceedings, Permafrost: the North American contribution to the Second International Conference, Yakutsk, USSR. National Academy of Sciences, Washington, pp. 447–453

Emmett, W.W., 1979. Overland flow. In: Kirby, M.J. (Ed.). Hillslope Hydrology, Wiley, Toronto, pp. 145–176 (chap. 5).

Farrell, R.E., Swerhone, G.D.W., van Kessel, C., 1991. Construction and evaluation of a reference electrode assembly for use in monitoring in situ soil redox potentials. Communications in Soil Science and Plant Analysis 22, 1059–1068.

Freeze, R.A., Cherry, J.A., 1979. Groundwater. Prentice-Hall, Englewood Cliffs, NJ (432pp).

Heginbottom, J.A., Radburn, L.K., 1992. Permafrost and ground ice conditions of Northwestern Canada. Geological Survey of Canada, Map 1691A, scale 1:1 000 000.

Hoag, R.S., Price, J.S., 1997. The effects of matrix diffusion on solute transport and retardation in undisturbed peat in laboratory columns. Journal of Contaminant Hydrology 28 (3), 193–205.

Ivanov, K.E., 1981. (Water movement in mirelands) (translated by Thomson, A., Ingram, H.A.P.). Vodoobmen v bolotnykh landshaftakh. Academic Press, Toronto (p. 276).

Ingram, H.A.P., 1978. Soil layers in mires: function and terminology. Journal of Soil Science 29, 224–227.

MacKay, J.R., 1980. The Origin of Hummocks, Western Arctic Coast, Canada. Canadian Journal of Earth Science 17, 996–1006.

Marsh, P., Pomeroy, J.W., 1996. Meltwater fluxes at an Arctic forest-tundra site. Hydrological Processes 10, 1383–1400.

National Research Council of Canada (NRC), 1988. Glossary of Permafrost and Related Ground-Ice Terms, Permafrost Subcommittee, Associate Committee on Geotechnical Research. Technical Memorandum no. 142, Ottawa.

National Wetlands Working Group (NWWG), 1988. Wetlands of Canada: Ecological Land Classification Series, no. 24. Sustainable Development Branch, Environment Canada, Ottawa, Ontario, and Polyscience Publications Inc., Montreal, Quebec, 452pp.

Quinton, W.L., Marsh, P., 1998. The influence of mineral earth hummocks on subsurface drainage in the continuous permafrost zone. Permafrost and Periglacial Processes 9, 213–228.

Quinton, W.L., Marsh, P., 1999a. A conceptual framework for runoff generation in a permafrost environment. Hydrological Processes 13, 2563–2581.

Quinton, W.L., Marsh, P., 1999b. Image analysis and water tracing methods for examining runoff pathways. Soil Properties and Residence Times in the Continuous Permafrost Zone. Integrated Methods in Catchment Hydrology — Tracer, Remote Sensing and Hydrometric Techniques. IUGG 1999 Symposium HS4, Burmingham, UK, July, 1999. IAHS Publ. no. 258, pp. 257–264.

Romanov, V.V., 1968. Hydrophysics of bogs. Israel Program for Scientific Translations, Jerusalem, 299pp.

Rouse, H., Ince, S., 1957. History of Hydraulics. Edwards Brothers, Ann Arbor, MI (269pp).

Todd, D.K., 1959. Wiley. Ground Water Hydrology. (p. 336).

Verry, E.S., Boelter, D.H., 1978. Peatland hydrology. In: Greeson, P. (Ed.), Wetland Functions and Values: the State of Our Understanding. Proceedings of the National Symposium on Wetlands. Lake Buena Vista, Florida, November 7–10. Minneapolis, MN, American Water Research Association, pp. 389–402.